 ation information: DOI 10.1109/TPWRD.2016.2638544, IEEE

Accelerated Zone II Operation of Distance Relay Using Impedance Change Directions

Sadegh Vejdan, *Student Member, IEEE,* Majid Sanaye-Pasand, *Senior Member, IEEE, and* Tarlochan S. Sidhu, *Fellow, IEEE*

***Abstract*—Legacy distance protection introduces an intentional delay before the trip command for Zone 2 internal faults. Instantaneous fault clearance in such faults can be achieved if distance relays are equipped with reliable communication. However, communication channel is not available or enabled in some lines. Besides some channels are prone to faults occurred on the line degrading their reliability. To overcome such drawbacks in instantaneous fault clearance, a local algorithm is proposed that uses the relay local signals to accelerate the trip for Zone 2 internal faults. The change in the relay seen impedance resulted by remote circuit breaker operation (RCBO) is the decision criterion in this method. The related impedance change equations are analytically derived and formulated. It is shown that the proposed method outperforms the similar approaches and improves their shortcomings in light- and no-load conditions and zero resistance faults. While most of the methods in literature are not sensitive enough to detect single-phase RCBO which is common during single-phase transient faults, significant improvement is attained by the proposed method in this regard. Performance of the proposed method is investigated under various fault and system conditions. Simulation results disclose high reliability of the proposed algorithm during all these conditions.**

***Index Terms*— Accelerated operation, Backup protection, Distance relay, Transmission line protection.**

I. Introduction

SCRUTINIZING major blackouts that have happened all around the world clearly demonstrate that wrong or delayed operation of protective relays is one of the main causes of these events [1]. Thus, fast and secure removal of the fault can contribute to substantial benefits from system, equipment and consumer points of view.

Distance relays are the main and the most common protective elements of transmission line protection. Despite their remarkable performance, they also show some drawbacks, e.g. the inability to provide instantaneous operation for remote end faults. This is compensated by using a communication link between two terminals of the transmission line called tele-protection system (TPS) [2]. TPS is utilized in pilot protection schemes to accelerate the protective decisions [3]–[6]. However, some transmission lines are not equipped with such systems. Also communication link failure, its delay and inappropriate setting are inevitable which reduce protective system reliability. Thus, it is required to use local non-communication algorithms, parallel to communication-based schemes to cover all the line length with minimum delay of fault clearance. This can be achieved by acceleration of distance relay second zone operation for internal faults.

Different non-communication approaches have been proposed in the literature, providing accelerated operation of distance relay for internal faults. These approaches can be classified based on their decision criteria that are sound phase current magnitudes [7] and [8], sequence current/voltage magnitudes [9]–[14], high frequency components [15]–[21], impedance/reactance change [22] and [23] and active/reactive power change [24]. Nearly all these algorithms are proposed to detect remote circuit breaker operation (RCBO) using the aforementioned criteria. Algorithms in [7] can detect a three-phase RCBO during an unbalanced internal fault since sound phase currents can change from load current to open circuit current. Special measures must be taken to discriminate between RCBO and light load situation using these algorithms. Detecting changes in negative and zero sequence currents resulted by a breaker operation are proposed in [9] and [10] to accelerate the relay delayed operation for internal faults. Faults are classified internal as far as these detected changes during the faults occur in the second zone. While too sensitive for both internal and external faults, these methods show less sensitivity for line to line faults due to absence of zero sequence component. Thus, an accelerated zone is introduced in [11] covering the last 20 percentage of the line length. However, this zone may not be applied practically due to instrument transformer errors.

BO schemes are proposed in [12] and [13] as delayed and instant operation approaches based on identical criteria of sequence currents and voltages, respectively. The delayed approach includes a constant time delay by which the sequence currents criterion must not decrease a threshold setting providing that the fault is internal. Otherwise, an external breaker operation is detected and hence the accelerated trip (AT) command is not issued. This approach shows deficiency in case of a delayed breaker operation and may accelerate the trip for such external fault scenarios. To overcome such defect the instant operation approach is introduced that relies on AT for all faults occurred in the accelerated zone. Monitoring the sequence voltage criterion can discriminate internal and external faults followed by a reclosing scheme for external ones. This approach may endanger the system stability due to the outage of many lines connected to the faulted line terminals. Another algorithm is

This work was supported by the University of Tehran under Grant No. 8101064-1-09.

The first two authors are with the School of Electrical and Computer Engineering, College of Engineering, University of Tehran, Tehran 14395-515, Iran (e-mail: vejdan@ut.ac.ir; msanaye@ut.ac.ir). T. S. Sidhu is with the University of Ontario Institute of Technology, Oshawa, ON L1H 7K4 Canada (email: Tarlochan.Sidhu@uoit.ca)

 ation information: DOI 10.1109/TPWRD.2016.2638544, IEEE

proposed in [14] based on the modal transformation introducing novel quantities with high sensitivity at the cost of increased complexity.

Other algorithms utilize analysis of high frequency components such as wavelet to detect RCBO [15]. High sensitivity can be achieved while these methods need special wideband instrumentations with high sampling rates. Also the extra computational burden can limit their implementation on conventional protective systems. The seen reactance and impedance are also subject to change as a result of RCBO. A three-phase RCBO results in a change in the sound phase reactances from the load value to capacitive charging as suggested in [23]. Furthermore, the faulted phase impedance is shown in [22] to converge to a specific area in the R-X plane. Application of this method is limited also in case of low pre-fault power flow as well as low fault resistance value. It is shown in [24] that RCBO can change the X/R ratio seen by the local relay as well as the change in active and reactive powers. This method cannot provide AT during light load conditions.

The previous methods provided valuable algorithms and results while their performance can be still improved. A novel accelerated trip algorithm is proposed in this paper that can be used in more general conditions and cover the previous methods shortcomings. This method is based on the impedance change directions seen by different impedance measurement units of distance relay, i.e. phase-to-ground and phase-to-phase units. The proposed algorithm utilizes two parallel units each one is designed whether for high or low fault resistance cases. The operation setting of each unit is overlapped with the other one to ensure a reliable operation for a wide range of fault resistances. The limited operation of previous algorithms in low load conditions is improved using the proposed one. Another contribution of this algorithm is the reliable detection of single-phase RCBO that is a part of the prevalent auto-reclosing scheme during transient single-phase faults. Secure operation for transient phenomena resulting in identical impedance changes is guaranteed by application of efficient blocking units. Various simulation results have demonstrated the fast and secure operation of the proposed AT algorithm.

II. Problem Description and Proposed Method

Distance relays provide great selectivity comparing to other protective relays. However, the limited accuracy of instrumentation transformers (CT and CVT) accompanied by relay errors impose safety margins on zone settings for the sake of coordination with other distance relays. As a result, a typical 20% margin is applied. Thus, the relay first zone covers only 80% of the line length, instantaneously. Since transmission lines are protected from both ends, only 60% of the line length can be protected instantaneously. It should be noted that fault resistance can decrease the real two-sided instantaneous operation range to even less than a half.

For the typical case shown in Fig. 1, fault is removed from one side instantaneously while removal from the other side is delayed by zone 2 time setting. However, operation of R2 can

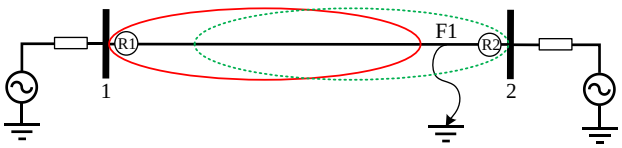

Fig. 1. A two-sided protected transmission line

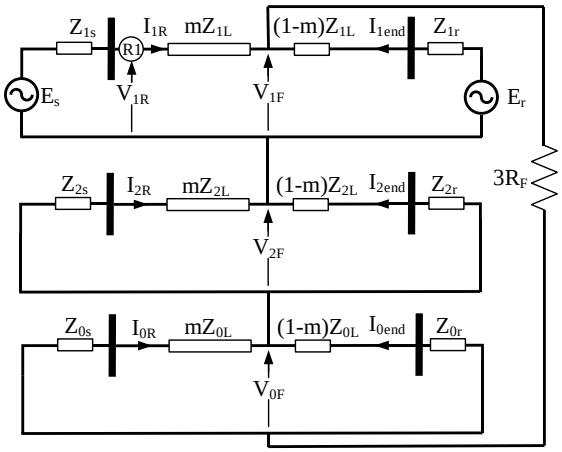

Fig. 2. Equivalent network circuit during a single-phase fault

be detected by measuring the impedance change in specific directions to accelerate the operation of R1. The impedance change in phase-to-ground and phase-to-phase units are formulated and derived in the following.

A. Impedance Change Seen by Faulted Phase-to-Ground Unit

The equivalent network during a single-phase-to-ground fault can be described as shown in Fig. 2. In this figure, *m* is the fault location as a portion of line length. The relay seen impedance (Z_A) is calculated by:

$$Z_A = V_{AR} / (I_{AR} + K_0 I_{0R}) \quad (1)$$

where V_{AR}, I_{AR} and I_{0R} are phase A voltage, current and zero-sequence current at the relay location, respectively. Also, zero sequence compensation factor K_0 is defined as $(Z_{0L} - Z_{1L}) / Z_{1L}$ with Z_{1L} and Z_{0L} being positive and zero sequence impedances of the line, respectively. The faulted phase A voltage at the relay location (V_{AR}) can be written in terms of positive, negative and zero sequence voltages at the relay location (V_{1R} ,V_{2R} ,V_{0R}) as below:

$$\begin{aligned} V_{AR} &= V_{1R} + V_{2R} + V_{0R} \\ &= (V_{1F} + mZ_{1L} I_{1R}) + (V_{2F} + mZ_{2L} I_{2R}) + (V_{0F} + mZ_{0L} I_{0R}) \end{aligned} \quad (2)$$

where V_{1F}, V_{2F} and V_{0F} are positive, negative and zero sequence voltages at the fault location, respectively. *m* denotes the fault location as a portion of the line length ($0<m<1$) and Z_{2L} is the negative sequence impedance of the line. Similarly, I_{1R} and I_{2R} are positive and negative currents at the relay location, respectively.

KVL in outer loop of Fig. 2 yields:

$$V_{AF} = V_{1F} + V_{2F} + V_{0F} = 3R_F I_{1F} \quad (3)$$

where V_{AF}, R_F and I_{1F} are fault voltage, resistance and positive sequence current, respectively.

Positive and negative sequence line impedances are assumed to be equal, i.e. $Z_{1L} = Z_{2L} \neq Z_{0L}$. Hence (3) becomes:

 ation information: DOI 10.1109/TPWRD.2016.2638544, IEEE

$$V_{AR} = V_{AR} + mZ_{1L}I_{0R} - mZ_{1L}I_{0R}$$
$$= mZ_{1L}(I_{1R} + I_{2R} + I_{0R} + I_{0R}((Z_{0L} - Z_{1L})/Z_{1L})) + 3R_F I_{1F} \quad (4)$$

The faulted phase current is expressed as:

$$I_{AR} = I_{1R} + I_{2R} + I_{0R} \quad (5)$$

where the relay sequence currents can be calculated using a current division at the fault point.

$$I_{(1,2,0)R} = C_{(1,2,0)}I_{(1,2,0)F} \quad (6)$$

Current distribution factor (C) is defined as the portion of fault current flowing through the line terminal where the relay is located.

$$C_1 = \frac{E_s - E_r}{I_{1F}(Z_{1s} + Z_{1L} + Z_{1r})} + \frac{(1-m)Z_{1L} + Z_{1r}}{Z_{1s} + Z_{1L} + Z_{1r}} \quad (7)$$

$$C_{(2,0)} = \frac{(1-m)Z_{(2,0)L} + Z_{(2,0)r}}{Z_{(2,0)s} + Z_{(2,0)L} + Z_{(2,0)r}} = \beta_{(2,0)}e^{j\theta_{(2,0)}};\ \theta_{(2,0)} \simeq 0 \quad (8)$$

where E_s and E_r are the sending and receiving end source voltages and $Z_{(1,2,0)s}$ and $Z_{(1,2,0)r}$ are their positive/negative/zero sequence, respectively.

Besides, it can be shown that in a single-phase-to-ground fault, all fault sequence currents are equal to one third of the faulted phase current. Thus, the fault current seen by the relay is:

$$I_{AR} = (C_1 + C_2 + C_0)I_{1F} \quad (9)$$

Finally, the seen impedance, that is a function of fault location and resistance, would be:

$$Z_A = mZ_{1L} + 3R_F/(C_1 + C_2 + C_0(1+K_0)) \quad (10)$$

In no-load condition (E_s=E_r), it is trivial to see that C_1 is almost a real value. In fault calculations, the network is considered to be almost pure inductive. This is highly consistent with practical cases in transmission lines where the reactance (X) is high due to large phase spacing and the resistance (R) is low for lowering the losses. Higher X/R ratio makes this assumption more accurate. Moreover, system is deemed as homogenous with Z_0/Z_1 equal for both the line and the rest of the network, as in [25].

As a result, current distribution factors are considered equal.

$$C_1 = C_2 = C_0 = \frac{(1-m)Z_{(1,2,0)L} + Z_{(1,2,0)r}}{Z_{(1,2,0)s} + Z_{(1,2,0)L} + Z_{(1,2,0)r}} \quad (11)$$

This way, the relay sequence currents are equal $I_{1R} = I_{2R} = I_{0R}$ and the seen impedance is:

$$Z_A = mZ_{1L} + \frac{3R_F I_{1F}}{(3+K_0)I_{1R}} = mZ_{1L} + \frac{R_F}{1+K_0/3}\cdot\frac{I_{1F}}{I_{1R}} \quad (12)$$

It should be noted that I_{1F} and I_{1R} currents are in phase in no-load condition since C is assumed to be real.

Single-pole tripping of the remote end circuit breaker changes the configuration of the equivalent circuit to what shown in Fig. 3. The observed changes are due to imposed physical conditions where the voltages across the closed breaker poles are zero as well as the remote end injected fault current of the opened pole [26].

$$\left.\begin{aligned} V_{CB-B} = V_{CB-C} = 0 \\ V_{CB-A} = V_{CB} \end{aligned}\right\} \Rightarrow V_{CB1} = V_{CB2} = V_{CB0} = \frac{V_{CB}}{3} \quad (13)$$

$$I_{Aend} = 0 \Rightarrow I_{1end} + I_{2end} + I_{0end} = 0 \quad (14)$$

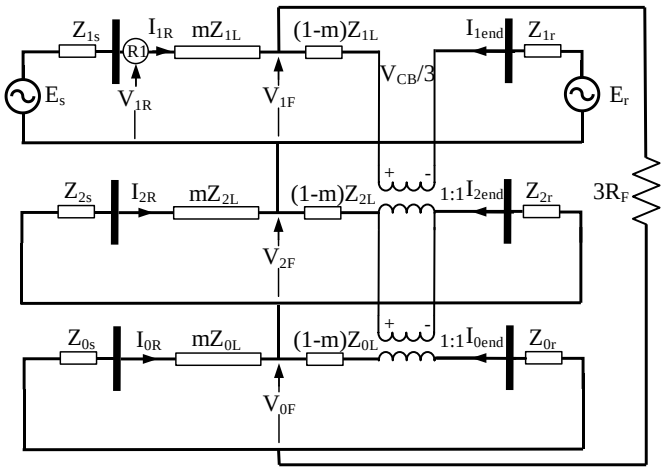

Fig. 3. Equivalent network circuit during a single-phase fault after RCBO

where $V_{CB-(A,B,C)}$ and $V_{CB(1,2,0)}$ are the voltages across the remote circuit breaker for each phase and each sequence, respectively. Also, I_{Aend} denotes the remote circuit breaker current of phase A that is zero after breaker operation. These changes cause the current distribution factors not be equal anymore. Hence, the calculated impedance after RCBO in the faulted phase A (Z_A^{RCBO}) is:

$$Z_A^{RCBO} = mZ_{1L} + 3R_F I_{1F}/(I_{1R} + I_{2R} + I_{0R}(1+K_0)) \quad (15)$$

The fault current is only supplied by one end of transmission line:

$$3I_{1F} = I_{1F} + I_{2F} + I_{0F}$$
$$= (I_{1R} + I_{1end}) + (I_{2R} + I_{2end}) + (I_{0R} + I_{0end}) = I_{1R} + I_{2R} + I_{0R} \quad (16)$$

Thus, Z_A^{RCBO} can be calculated by:

$$Z_A^{RCBO} = mZ_{1L} + \frac{R_F(I_{1R} + I_{2R} + I_{0R})}{I_{1R} + I_{2R} + I_{0R}(1+K_0)} \quad (17)$$

Neglecting the small angle of K_0, it can be shown that the impedance change caused by RCBO is approximately a reduction in its real part. The proof is provided in Appendix. Detection of impedance change in this direction is the principle of the proposed AT scheme.

To generalize the derived formulation in loaded conditions ($E_s \neq E_r$), it is proposed to use the pure fault current that is the fault current minus the load current. This current is also referred to as "superimposed" or "incremental" current that is deployed in other online protection applications as in [27], [28]. It should be mentioned that this current is only used for calculating the impedance change and not the instantaneous impedance.

B. Impedance Change Seen by Faulted Phase to Sound Phase Unit

As observed, impedance change in the faulted phase is proportional to the fault resistance. Hence, in case of low resistance faults, another measure should be taken to detect RCBO. Thus, it is proposed to detect changes in the impedance seen by faulted-to-sound-phase units that are shown to have acceptable sensitivity. The goal is to find the impedance change direction caused by RCBO. The seen impedance of AB unit can be calculated during a single-phase

 ation information: DOI 10.1109/TPWRD.2016.2638544, IEEE

(A-to-ground) fault using the following equations. Phase B voltage (V_{BR}) and current at the relay location (I_{BR}) can be calculated in the same way as phase A:

$$V_{BR} = \alpha^2(V_{1F} + mZ_{1L}I_{1R}) + \alpha\,(V_{2F} + mZ_{2L}I_{2R}) + (V_{0F} + mZ_{0L}I_{0R}) \quad (18)$$

$$I_{BR} = \alpha^2 I_{1R} + \alpha I_{2R} + I_{0R} \quad (19)$$

where $\alpha = \exp(j2\pi/3)$.

The line to line voltage (V_{AB}) can then be calculated as:

$$V_{AB} = V_{AR} - V_{BR} =$$
$$(1-\alpha^2)(V_{1F} + mZ_{1L}I_{1R}) + (1-\alpha)(V_{2F} + mZ_{2L}I_{2R}) =$$
$$(1-\alpha^2)mZ_{1L}I_{1R} + (1-\alpha)mZ_{2L}I_{2R} + (1-\alpha^2)V_{1F} + (1-\alpha)V_{2F} \quad (20)$$

V_{1F} can be expressed as:

$$V_{1F} = 3R_F I_{1F} - V_{2F} - V_{0F} \quad (21)$$

Knowing the difference between phase A and B currents (I_{AB}) as $I_{AB} = I_{AR} - I_{BR} = (1-\alpha^2)I_{1R} + (1-\alpha)I_{2R}$, V_{AB} is:

$$V_{AB} = mZ_{1L}(I_{AB}) + (\alpha^2 - \alpha)V_{2F} + (\alpha^2 - 1)V_{0F} + (1-\alpha^2)3R_F I_{1F} \quad (22)$$

where $V_{2F} = (-I_{2R})(Z_{2s} + mZ_{2L})$ and $V_{0F} = (-I_{0R})(Z_{0s} + mZ_{0L})$.

The line to line seen impedance (Z_{AB}) can be expressed as (23) using only the signals at the relay location:

$$Z_{AB} = mZ_{1L} + [(\alpha^2 - \alpha)(-I_{2R})(Z_{2s} + mZ_{2L}) + (\alpha^2 - 1)(-I_{0R})(Z_{0s} + mZ_{0L}) + (1-\alpha^2)3R_F I_{1F}]/[(1-\alpha^2)I_{1R} + (1-\alpha)I_{2R}] \quad (23)$$

Positive and negative sequence currents at the relay location are equal in no-load condition meaning that:

$$I_{1R} = I_{2R} \Rightarrow (1-\alpha^2)I_{1R} + (1-\alpha)I_{2R} = (2-\alpha^2-\alpha)I_{1R} = 3I_{1R} \quad (24)$$

Since $\alpha^2 - \alpha = \sqrt{3}\angle -90^\circ$ and $\alpha^2 - 1 = \sqrt{3}\angle -150^\circ$, the impedance can be decomposed into terms each with different phase angle as below:

$$Z_{AB} = mZ_{1L} + (1/\sqrt{3})(Z_{2s} + mZ_{2L})\angle 90^\circ + [(1/\sqrt{3})(Z_{0s} + mZ_{0L})(I_{0R}/I_{1R}) + \sqrt{3}R_F(I_{1F}/I_{1R})]\angle 30^\circ \quad (25)$$

Similarly, for phase C to A, the seen impedance (Z_{CA}) is:

$$Z_{CA} = mZ_{1L} + (1/\sqrt{3})(Z_{2s} + mZ_{2L})\angle -90^\circ + [(1/\sqrt{3})(Z_{0s} + mZ_{0L})(I_{0R}/I_{1R}) + \sqrt{3}R_F(I_{1F}/I_{1R})]\angle -30^\circ \quad (26)$$

The loci of these impedances are shown in Fig. 4. These impedances each has two constant terms $mZ_{1L} + (1/\sqrt{3})(Z_{2s} + mZ_{2L})\angle \pm 90^\circ$. Therefore, no change occurs in those due to RCBO while the other two terms $[(1/\sqrt{3})(Z_{0s} + mZ_{0L})(I_{0R}/I_{1R}) + \sqrt{3}R_F(I_{1F}/I_{1R})]\angle \pm 30^\circ$ change in specific directions in the R-X plane. Unlike phase-to-ground impedance change, the change in line to line impedances is not just dependent on fault resistance. Hence, the impedance change in the direction which the term $(1/\sqrt{3})(Z_{0s} + mZ_{0L})(I_{0R}/I_{1R})\angle \pm 30^\circ$ changes can be measured to detect RCBO while the fault resistance is low and phase-to-ground unit has low sensitivity. Accordingly, R_F is assumed negligible to find the impedance change direction in these units. As previously mentioned, in no-load condition,

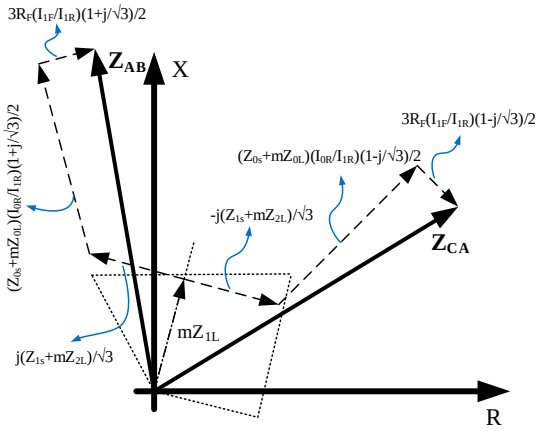

Fig. 4. Phase-to-phase impedance loci during a single-phase fault

sequence currents at the relay location (I_{1R} and I_{0R}) are in phase before RCBO. It is also shown in Appendix that these currents remain fairly in phase after RCBO while I_{0R}/I_{1R} decreases. Thus, the impedance change direction is known for both AB and CA units and can be computed when zero sequence impedance angle is available. Considering $\angle(Z_{0s} + mZ_{0L}) = 75^\circ$, impedance change for AB and CA units are in the opposite direction of $\angle(Z_{0s} + mZ_{0L}) \pm 30^\circ$ due to the decrease in I_{0R}/I_{1R} ratio. This yields to the angles of $75^\circ + 30^\circ - 180^\circ = -75^\circ$ and $75^\circ - 30^\circ - 180^\circ = -135^\circ$ for AB and CA units, respectively, as illustrated in Fig. 5.

The impedance changes in these directions following a single-phase fault are calculated and compared to a threshold to detect a possible RCBO. Since a significant impedance change in any direction may incorrectly meet the condition above, the specified change in that direction is compared to the absolute value of impedance change to insure that the change is mainly in the predetermined direction. This justifies the operation zones geometry in Fig. 5 which are limited by an angle with respect to the predetermined directions. It is worth noting that using pure fault current, instead of faulted phase current, in impedance change calculation can greatly estimate any pre-fault load condition with no-load results.

In high-resistance faults followed by RCBO, the direction deviates from solid fault condition. This makes the calculated impedance changes to be less and may reduce the sensitivity. However, single-phase-to-ground units can detect RCBO in these faults. Overlapping these units can extend the fault resistance range for the proposed AT algorithm from solid faults to high-resistance ones.

The flowchart of the proposed algorithm is illustrated in Fig. 6. It is comprised of three stages i.e. activation, tripping and blocking. Following a single-phase fault, phase impedance change is calculated in the first stage. This is done to ensure that transient impedance change due to fault occurrence and sampling errors does not trigger the algorithm. Accordingly, impedance should be settled for a specified time and its change should be less than a setting in order to activate the second stage. It is important that the time setting should be less than the minimum possible RCBO time and the impedance setting be greater than instrumentation accuracy. In the rare case of very large transients and sampling errors, the

 ation information: DOI 10.1109/TPWRD.2016.2638544, IEEE

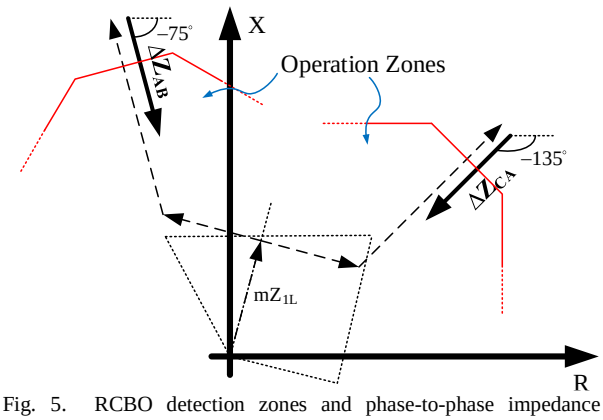

Fig. 5. RCBO detection zones and phase-to-phase impedance change direction resulted by RCBO in a low resistance single-phase fault

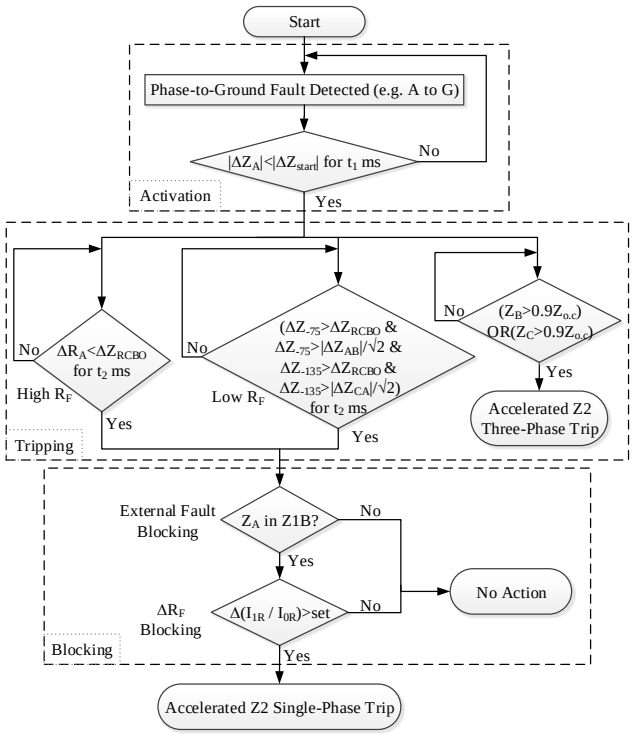

Fig. 6. The flowchart of the proposed algorithm

impedance change does not settle and therefore the algorithm is not activated while the input signals are unreliable. Accordingly, the conventional zone 2 operates and no insecure accelerated trip will be issued.

In the second stage, three units perform in parallel. One is designed to detect a three-phase RCBO by checking sound phase impedances. These impedances become equal to their large open circuit value in a single-phase fault followed by a three-phase RCBO. If the sound impedance magnitudes are greater than 90% of their open circuit value, a three-phase accelerated trip command is issued accordingly. In the other two units, the net impedance changes along the predefined directions are calculated simultaneously in the faulted phase and also in faulted to sound phases. These two units operate in parallel and it is sufficient that either of them can detect RCBO regardless of the R_F value. The output of these two units are combined with an OR logic gate so that the algorithm can cover both low and high R_F faults. The names "High R_F" and "Low R_F" in Fig. 6 are given just because the unit output is more sensitive to a high/low R_F and it can detect RCBO better in that range of fault resistance.

As discussed, pure fault current is used in these calculations as:

$$\tilde{I}_{PureFault}(k) = \tilde{I}_{Fault}(k) - \tilde{I}_{PreFault} \quad (27)$$

where $\tilde{I}(k)$ is the current phasor at the kth sample and $\tilde{I}_{PreFault}$ is fixed to the current phasor half-cycle before fault inception.

The third stage is designed to enhance the security of the proposed algorithm against phenomena other than RCBO which may result in similar impedance changes.

Discrimination of internal and external faults in this stage is carried out by checking whether the faulted impedance is in the extended zone 1 (Z1B) as in [9]-[11]. Unlike the previous methods, the proposed algorithm can be activated even if the pre-RCBO impedance is out of Z1B. This usually happens due to fault high resistance and strong infeed effect. Thus, the proposed algorithm can operate for a wider fault resistance range and is less sensitive to zone 2 setting. Furthermore, sudden change in fault resistance may trigger the tripping stage that is blocked by checking the positive to zero sequence pure fault current ratio. The value of this ratio for the first 10 ms right after the activation time of the algorithm (end of stage 1) is averaged and taken as the reference. This value is stored in the memory and continuously compared with the I_{1R}/I_{0R} ratio calculated for the next samples. In case a trip command is issued by the second stage, the instantaneous value of I_{1R}/I_{0R} ratio should be greater than the reference value by a threshold, otherwise the trip signal is blocked. As discussed in Appendix, this ratio does not change significantly with the change in fault resistance while it does so following RCBO.

III. Simulations and Results

The performance of the proposed algorithm has been tested under various fault and system conditions. A three-machine system has been simulated as in Fig. 7 using PSCAD/EMTDC with the parameters given in Appendix. The line under study is protected with one distance relay at each end with zone 1 setting of 80% of the line length. A single-phase fault occurs on the last 20% covered by zone 1 of R2 and zone 2 of R1. R2 is implemented in PSCAD/EMTDC in order to simulate RCBO. Phasors are derived in PSCAD/EMTDC with the sampling rate of 1 kHz using DFT method and then imported to MATLAB where the proposed method is implemented. Several parameters are tested to verify the reliability of the accelerated zone 2 algorithm of R1. These include fault resistance, load flow, system impedances, external faults and some transient phenomena. A subsection of comprehensive comparison between the proposed method and the previous approaches follows these results.

A. Fault Resistance

As discussed in the previous section, the algorithm is designed to operate for both low and high fault resistance conditions. The seen impedances by R1 is depicted in Fig. 8 (a) and (b) where a single-phase (AG) fault occurs at 90% of the line length with R_F equal to 20 and 0 Ω, respectively. The

 ation information: DOI 10.1109/TPWRD.2016.2638544, IEEE

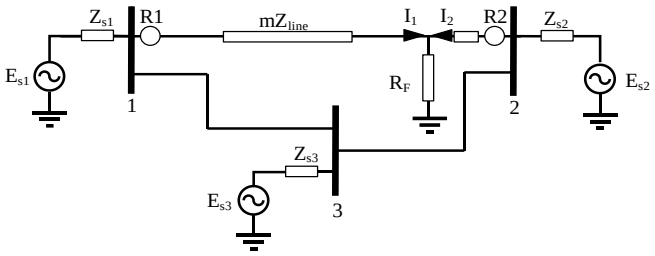

Fig. 7. Single line diagram of the simulated system

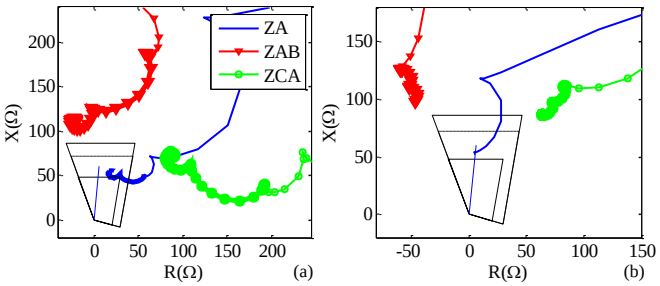

Fig. 8. Impedance trajectories for (a) high- and (b) low-resistance faults

bolded impedance trajectories denote the impedance after RCBO. These results are completely congruent with what expected in terms of impedance change caused by RCBO. The impedance change of the faulted phase for a high-resistance fault is almost in the opposite direction of R (i.e. -R) while for a solid fault it is trivial. However, the impedance change of faulted-to-sound phase units for solid faults are almost in phase with -75 and -135 angles. Accordingly, for these two scenarios, AT is issued in just 13 and 57 ms, respectively, after the faulted impedance enters zone 2. It is worth mentioning that for the high-resistance fault case, unlike solid fault, the faulted impedance does not enter zone 2 before RCBO. This is why the trip time minus the time when the impedance enters zone 2 (t Z2) is much less in this case. Comparing to the conventional zone 2 time setting of hundreds of milliseconds, the improvement in both cases is significant.

The algorithm is tested for a wide range of fault resistances from solid faults to those with R_F of almost 2/3 of zone 1 setting. Operation times in ms are provided in Table I. The trip time is determined by the fault incidence time (t fault, as an initial value) plus delays in the activation stage (controlled by timer t_1 in Fig. 6) plus delays in the tripping stage (controlled by t_2 in Fig. 6). The blocking stage is supposed to introduce negligible delay that is less than the sampling period (1 ms). It is apparent that low- and high-impedance units have overlap which increases the algorithm dependability. The previously proposed methods do not operate in high-resistance faults and their R_F coverage is much less than that of the proposed algorithm. In those algorithms, the faulted phase impedance should be seen inside Z1B before and after any possible RCBO. However, the proposed algorithm just checks this condition to be true before the trip is issued. This way, it can accelerate the trip and extend the R_F range to more than three times compared to the previous ones. For the faults with R_F>32 Ω the impedance seen by R2 is no longer in its first zone. Consequently, it will not operate instantaneously and similar to other methods both relays will operate after zone 2 time delay.

TABLE I
DIFFERENT OPERATION TIMES FOR VARIOUS FAULT RESISTANCES

R_F(Ω)	t fault (ms)	t Z2 (ms)	t RCBO (ms)	t trip AG (ms)	t trip AB/CA (ms)	t trip - t Z2 (ms)
0	205	220	255	-	277	57
2	205	220	255	-	276	56
4	205	221	255	-	276	55
6	205	221	256	288	274	53
8	205	222	256	282	274	52
10	205	224	264	289	-	65
15	205	271	265	287	-	16
20	205	273	266	286	-	13
25	205	275	267	284	-	9
30	205	292	272	293	-	1
32	205	302	283	303	-	1

Needless to say that application of the proposed algorithm is not just confined to the last 20% of the line whereas high-resistance faults occurring in zone 1 of one relay may be seen in the second zone with delayed operation. It is enough that only one of these relays detect the fault in its first zone.

B. Pre-fault Condition

It is proposed that the validity of the derived equations for impedance change is held under loaded and unbalanced systems by using pure fault currents. Accordingly, numerous pre-fault load conditions are tested that verify this proposition. Two scenarios with positive and negative power flows are reported for instance. In the first one, power flows from E_{s1} to E_{s2} with the voltage angle difference of $+30^\circ$. Fault occurs on 90% of line length and R_F is 20 Ω. The resulted impedance trajectories using pre-fault current is presented in Fig. 9(a). Again the change in the faulted phase impedance is in –R direction. The AT time is 17 ms.

Negative power flow is simulated in the second scenario in which E_{s1} lags E_{s2} by 30°. Fault is on 90% with R_F=0 Ω. In this case, shown in Fig. 9(b), AB and CA impedances change enough in the pre-known directions to activate AT after 54 ms. Extensive scenarios with different pre-fault load flow angles and fault resistances are simulated and summarized in Table II. This table provides the fault resistance range covered by the proposed algorithm for each power flow angle. It is seen that the algorithm can be applied to both lightly and heavily loaded systems over a wide range of R_F. It should be considered that larger angle differences is not a common case in power systems due to stability issues.

Algorithm performance under unbalanced pre-fault conditions is also tested similarly by adding unbalanced load to the system. The results for unbalanced conditions up to where I_0=I_2=0.2I_1 are similar to those in the balanced ones reported in Table II. This is expected since the algorithm decision is based on pure-fault currents that eliminates the effect of unbalanced conditions. It should be mentioned that a more unbalanced case is not practical in transmission lines.

C. System Impedances

The effect of source and line impedances as well as the line angle are discussed in this subsection. Different impedance values represent the source strength or weakness and also the

ation information: DOI 10.1109/TPWRD.2016.2638544, IEEE

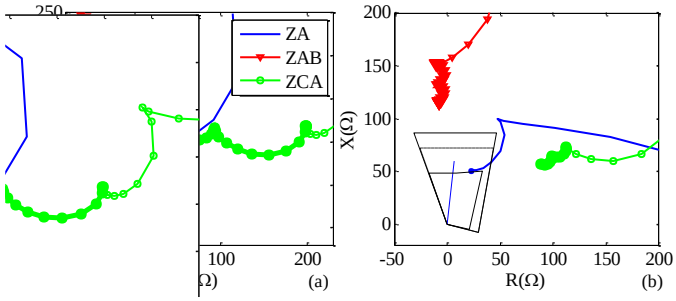

Fig. 9. Impedance trajectories during (a) positive and (b) negative load flow

TABLE II
FAULT RESISTANCE COVERAGE FOR DIFFERENT POWER FLOW ANGLES

δ (deg)	R_F (Ω)	δ (deg)	R_F (Ω)
-5	[0-32]	5	[0-34]
-10	[0-32]	10	[0-34]
-15	[0-32]	15	[0-35]
-20	[0-33]	20	[0-35]
-25	[0-34]	25	[0-35]
-30	[0-34]	30	[0-36]
-35	[0-35]	35	[0-36]

line length. Moreover, the line angle is determined by X/R ratio. A sensitivity analysis is performed on the fault resistance coverage of the proposed algorithm with respect to different line lengths as well as source capacities and the results are provided in Table III. It can be seen that both high R_F (faulted phase impedance change) and low R_F (sound-to-faulted phase impedance change) units overlap for a wide range of line lengths. Results also disclose a wider R_F coverage for shorter lines and stronger sources. Furthermore, different line angles are tested and the results for a 100 km line are reported in Table IV. It is clear that the proposed algorithm performs reliably for a wide range of line angles common in transmission level while it outperforms in higher X/R ratios.

D. External Faults

Discriminating internal and external faults is a crucial feature of the proposed algorithm that determines its security. Following a possible RCBO detection, the algorithm controls this feature by checking the faulted impedance to be in Z1B (120% of line impedance) as depicted in Fig. 6. An external fault results in the next line CB operation. Subsequently, the faulted impedance will be removed from R1 zones and it will not operate. In case of failure in the next line protection operation, no impedance change is detected and the conventional zone 2 time delay is applied similar to the previous methods.

A sample impedance trajectory is shown in Fig. 10 for a solid fault occurring on 10% of the next line length (line 2-3 in Fig. 7) and followed by its nearest CB operation. Not only the impedance changes are in totally different directions, but also the faulted impedance is out of zones. It exits Z1B and zone 2 in 2 and 5 ms, respectively, after CB operation of the next line. This is true for all the external faults.

E. Fault Resistance Transients

Various transient changes in fault resistance have been simulated to test the effectiveness of the algorithm e.g.

TABLE III
FAULT RESISTANCE COVERAGE FOR DIFFERENT SYSTEM IMPEDANCES

Line Length (km)	Source SCC (kA)	R_F (Ω)		(Max(R_F)/Z1)×100
		High R_F unit	Low R_F unit	
10	50	[2.1-4.3]	[0-3.2]	179.2
30	50	[2.5-6.2]	[0-5.5]	86.1
50	50	[2.9-8.7]	[0-6.3]	72.5
100	50	[4.2-17.5]	[0-8.1]	72.9
150	50	[5.1-25.3]	[0-9.0]	70.3
200	50	[5.8-32.1]	[0-9.9]	66.9
200	40	[5.7-29.8]	[0-9.7]	62.1
200	30	[5.5-27.5]	[0-9.5]	57.3

TABLE IV
FAULT RESISTANCE COVERAGE FOR DIFFERENT LINE ANGLES

θ=Line Angle (deg)	X/R Ratio (tan(θ))	R_F (Ω)		(Max(R_F)/Z1) ×100
		High R_F unit	Low R_F unit	
90	∞	[3.6-20.1]	[0-9.3]	83.8
85	11.43	[4.0-18.6]	[0-8.5]	77.5
80	5.67	[4.2-18.3]	[0-8.3]	76.3
75	3.73	[4.7-15.5]	[0-7.9]	64.6
70	2.75	[6.1-11.3]	[0-7.0]	47.1

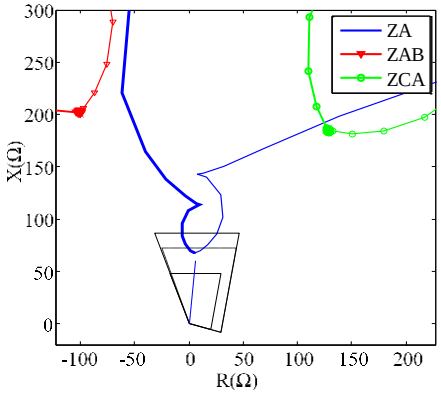

Fig. 10. Impedance trajectories for an external fault

variable R_F values during the fault and arcing. As previously stated, a sudden reduction in R_F can result in similar changes of the faulted impedance. Fig. 11 illustrates this case which R_F changes from 20 Ω to 1 Ω after fault occurrence. Using pure fault current, the impedance change is in –R direction and its magnitude is greater than the setting to detect a possible RCBO. Yet no considerable change is detected in I_{1R} / I_{0R} ratio that blocks the trip command in this scenario. This ratio is depicted in Fig. 12 and compared with the one during another scenario with RCBO. In both scenarios, a single-phase fault occurs on 90% of the line at t=210 ms. The algorithm activation time is t=231 ms. Hence the ratio reference value is 1.36 in both scenarios. In scenario *a*, R_F changes at t=250 ms, the high-R_F unit detects a possible impedance change at t=274 ms. The ratio value at this instant is 1.37. Since the change in the ratio is less than the threshold of 0.5, trip is blocked by the algorithm. In scenario *b*, RCBO occurs at t=263 ms and the trip is issued at t=286 ms. The ratio is equal to 2.42 at this instant and the change is greater than 0.5 that results in a trip. If R_F reduction is followed by RCBO, the algorithm can accelerate the trip. Also, while arcing faults tend to have increase in their resistance, these transients do not impair the proposed algorithm.

 ation information: DOI 10.1109/TPWRD.2016.2638544, IEEE

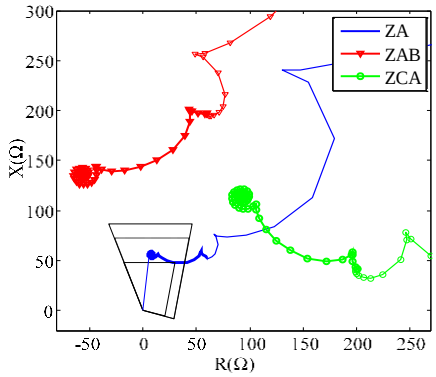

Fig. 11. Impedance trajectories during fault resistance reduction

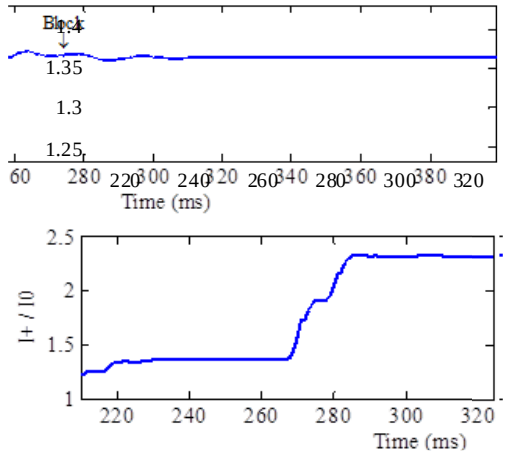

Fig. 12. Positive to zero sequence current ratio during (a) fault resistance reduction and (b) RCBO scenarios

F. Improvements and Comparison

To summarize the contributions of the proposed algorithm, a list of its capabilities and improvements is reported in Table V and compared to other local (non-communication based) RCBO detection methods. Previous methods in this Table are categorized based on their decision criteria as mentioned in the Introduction. This table clearly depicts the superiority of the proposed accelerated method that can be applied in more general system conditions to cover various single-phase faults with an improved reliability.

IV. Conclusion

A non-communication based accelerated operation of distance relay is proposed in this paper. The algorithm is designed to tackle the delayed fault clearance in case of communication unavailability or failure to improve the reliability of the protective system. Accordingly, remote circuit breaker operation is detected using an impedance change criterion. Respective formulation of the relay seen impedance discloses specific impedance changes in the R-X plane. Two different units for high and low fault resistances are implemented complementarily to cover a wide range of resistances and enhance the algorithm dependability. Furthermore, security of the algorithm is ensured by some blocking units discriminating RCBO from other similar events. Robustness of the proposed algorithm has been verified by numerous simulation scenarios. Outstanding improvements of the algorithm compared to the previous ones can be named as follows:

- Efficient sensitivity for single-phase RCBO detection
- Applicable to three-phase RCBO detection as well as single-phase
- Wide operation range of fault resistance
- Secure operation for different pre-fault load conditions
- Security enhancement under transients

Appendix
Proof of Impedance Change Direction caused by RCBO

Equation (13) shows that single-phase RCBO can be modeled by equal voltage sources in each equivalent sequence circuit (V_{CB}/3) as shown in Fig. 3. Thus, positive and zero sequence voltages at the fault location after RCBO ($V_{(1,0)F}$) can be written as:

$$V_{(1,0)F} = E_{(1,0)s} - (Z_{(1,0)s} + mZ_{(1,0)L})I_{(1,0)R} = E_{(1,0)r} + (V_{CB}/3) - [(Z_{(1,0)r} + (1-m)Z_{(1,0)L})(I_{(1,0)F} - I_{(1,0)R})] \quad \text{(A1)}$$

In three-phase balanced no-load condition $E_{1s} = E_{1r} = 1\angle 0^\circ$ and $E_{0s} = E_{0r} = 0$. Also, since $I_{1F} = I_{0F} = I_F$, the two above equations can be solved to find I_{0R} / I_{1R} ratio:

$$\frac{I_{0R}}{I_{1R}} = \frac{(1-m)Z_{0L} + Z_{0r} - (V_{CB}/3I_F)}{(1-m)Z_{1L} + Z_{1r} - (V_{CB}/3I_F)} \times \frac{Z_{1s} + Z_{1L} + Z_{1r}}{Z_{0s} + Z_{0L} + Z_{0r}} \quad \text{(A2)}$$

With negligible R_F, CB voltage is:

$$\left.\begin{aligned} V_{CB} &= V_{CB-A} = V_F - E_{r-A} \\ V_F &\simeq 0 \quad ; \quad E_{r-A} = 1\angle 0 \end{aligned}\right\} \Rightarrow V_{CB} = -1 \quad \text{(A3)}$$

TABLE V
Capabilities and Improvements of the Proposed Method Compared to Similar Approaches

Capability	Proposed Method	[7], [8]	[9]–[14]	[15]–[21]	[22]–[24]
Single phase RCBO detection	√	Only [8]	Only [12],[13]	√	Only [22]
Fault resistance coverage	From solid (R_F=0Ω) to out of zone 2†	[7] is independent of R_F, [8] only in zone 2	Only in zone 2	Independent of R_F	[22] low sensitivity for low R_F, [23], [24] independent of R_F
Pre-fault condition and load current coverage	Reliable in (un)balanced conditions and for all $I_{PreFault}$ values in single phase RCBO, $I_{PreFault}$>0.09I_{nom} in 3-phase RCBO	low sensitivity for low $I_{PreFault}$ values	Sensitive in unbalanced pre-fault condition	Secured	low sensitivity for low $I_{PreFault}$ values
Security against transients	Secured	Secured	Sensitive	Sensitive	[22] is sensitive in case of R_F change
No need of high frequency detectors	√	√	√	×	√
Reliable breaker failure operation and no intentional time delay	√	√	False for [12], [13]	√	√

†For large values of R_F that are outside zone 2 before RCBO and enter zone 2 after RCBO.

 ation information: DOI 10.1109/TPWRD.2016.2638544, IEEE

The fault current is also expressed as:

$$I_F = \frac{1\angle 0}{(Z_{1th} + Z_{2th} + Z_{0th})} \quad \text{(A4)}$$

The phase angle of I_{0R} / I_{1R} ratio after RCBO in (A2) can be estimated using (A3) and (A4):

$$\angle(I_{0R} / I_{1R})_{RCBO} =$$
$$\angle[\frac{(1-m)Z_{0L} + Z_{0r} + (Z_{1th} + Z_{2th} + Z_{0th})/3}{(1-m)Z_{1L} + Z_{1r} + (Z_{1th} + Z_{2th} + Z_{0th})/3} \times \frac{Z_{1s} + Z_{1L} + Z_{1r}}{Z_{0s} + Z_{0L} + Z_{0r}}]$$
$$\simeq 0^\circ = \angle(I_{0R} / I_{1R})_{noRCBO} \quad \text{(A5)}$$

where $\angle(I_{0R} / I_{1R})_{noRCBO}$ is the phase angle of I_{0R} / I_{1R} ratio before RCBO that can be derived using V_{CB}=0 in (A2). The result in (A5) shows that I_{0R} / I_{1R} ratio remains in phase before and after RCBO.

Furthermore, the reduction in the ratio magnitude is deduced as follows:

Take $a = (1-m)Z_{0L} + Z_{0r}$, $b = (1-m)Z_{1L} + Z_{1r}$, $c = (Z_{1th} + Z_{2th} + Z_{0th})/3$ and $k = \frac{Z_{1s} + Z_{1L} + Z_{1r}}{Z_{0s} + Z_{0L} + Z_{0r}} > 0$. The ratios can now be written as:

$$|(I_{0R} / I_{1R})_{noRCBO}| = |a/b||k| \quad \text{(A6)}$$

$$|(I_{0R} / I_{1R})_{RCBO}| = |(a+c)/(b+c)||k| \quad \text{(A7)}$$

Suppose $|(I_{0R} / I_{1R})_{RCBO}| < |(I_{0R} / I_{1R})_{noRCBO}|$ that is:

$$|(a+c)/(b+c)||k| < |a/b||k| \Rightarrow |a+c||b| < |b+c||a| \quad \text{(A8)}$$

Since all the terms are purely inductive, $|a+c| = |a| + |c|$ and $|b+c| = |b| + |c|$. The inequality in (A8) can be expressed as:

$$|a||b| + |c||b| < |b||a| + |c||a| \quad \text{(A9)}$$

None of the terms are zero and (A9) can be simplified to:

$$|b| < |a| \quad \text{(A10)}$$

that is true due to the fact that zero sequence impedance is greater than the positive one. Thus, the current ratio is reduced after RCBO.

Thus, the impedance change is in the direction that the term $(1/\sqrt{3})(Z_{0s} + mZ_{0L})(I_{0R} / I_{1R})\angle \pm 30^\circ$ reduces. Similar argument is valid to show that this ratio increases if CB of the next line operates due to an external fault. This way, a decrease in the inverse of this ratio (I_{1R} / I_{0R}) is used as a blocking criterion. The ratio I_{1R} / I_{0R} is also deployed to increase the security against a sudden decrease in R_F which may generate similar impedance change patterns. However, any change in R_F results in a change in each sequence current that is proportional to their impedances in no-load condition. Since the impedances are constant, the ratio does not change if the pure fault current is used.

TABLE AI
SIMULATED TRANSMISSION LINE PARAMETERS

R_+ (Ω/km)	XL_+ (Ω/km)	XC_+ (MΩ×km)	R_0 (Ω/km)	XL_0 (Ω/km)	XC_0 (MΩ ×km)
0.03	0.3	0.26	0.3	1.11	0.4

TEST SYSTEM PARAMETERS
Line lengths=200 km, Voltage=230 kV, Source SCRs=50 kA

ACKNOWLEDGEMENT

The first two authors would like to thank Mr. Seyyed Mohammad Hashemi for his help and comments.

REFERENCES

[1] P. Pourbeik, P. S. Kundur, and C. W. Taylor, "The anatomy of a power grid blackout", *IEEE Power & Energy Magazine*, vol. 4, no. 5, pp. 22-29, Sep. 2006.

[2] G. Ziegler, "Numerical Distance Protection: Principles and Applications", John Wiley & Sons, 2011.

[3] B. Li, F. Guo, X. Li, and Z. Q. Bo, "Circulating unbalanced currents of EHV/UHV untransposed double-circuit lines and their influence on pilot protection," *IEEE Trans. on Power Del.*, vol. 29, no. 2, pp. 825-833, 2013.

[4] J. Suonan, K. Liu, and G. Song, "A novel UHV/EHV transmission-line pilot protection based on fault component integrated impedance," *IEEE Trans. on Power Del.*, vol. 26, no. 1, pp. 127-134, 2011.

[5] J. Suonan, X. Deng, and K. Liu, "Transmission line pilot protection principle based on integrated impedance," *Gener., Transm. & Distrib., IET*, vol. 5, no. 10, pp. 1003-1010, 2011.

[6] S. M. Hashemi, M. Tarafdar Hagh, and H. Seyedi, "A novel backup distance protection scheme for series-compensated transmission lines," *IEEE Trans. on Power Del.*, vol. 29, no. 2, pp. 699-707, 2014.

[7] A. G. Phadke, S. H. Horowitz, "Adaptive relaying," *IEEE Computer Applications in Power*, vol. 3, no. 3, pp. 47-51 , 1990.

[8] A. Mahari, and M. Sanaye-Pasand, "An accelerated single-pole trip scheme for zone-2 faults of distance relays," *Accepted to be published in IEEE Trans. on Power Del. doi: 10.1109/TPWRD.2016.2555787.*

[9] C. Deshu, L. Pei, P. Hua, G. S. Hope, O. Malik, "Scheme for accelerated trip for faults in the second zone of protection of a transmission line," *IEEE Trans. on Power Del.*, vol. 4, no. 2, pp. 942-948, Apr. 1989.

[10] L. Pei, C. Deshu, P. Hua, O. Malik, and G. Hope, "Analysis of an accelerated trip scheme for faults in the second zone of protection of a transmission line," *IEEE Trans. on Power Del.*, vol. 5, no. 1, pp. 72-78. Mar. 1990.

[11] T. Sidhu, P. Ye, and M. Sachdev, "Accelerated trip scheme for second zone distance protection," *IEE Proceedings on Gener., Transm. & Distrib.*, vol. 5, no. 3, pp. 325-333, May 2003.

[12] Z. Q. Bo, "Adaptive non-communication protection for power lines BO scheme 1-The delayed operation approach", *IEEE Trans. on Power Del.*, vol. 17, no. 1, pp. 85-9 1 , Jan. 2002.

[13] Z. Q. Bo, "Adaptive non-communication protection for power lines, BO scheme 2—The instant operation approach," *IEEE Trans. on Power Del.*, vol. 17, no.1, pp. 92–96, Jan. 2002.

[14] H. Darwish, T. Kaway, A. Taalab, O. Malik, "Robust non-communication line protection scheme using novel quantities", *IEEE Trans. on Power Del.*, vol. 2, no. 6, 2006.

[15] T. Shi, H. Zhang, P. Liu, D. Zhang, Q. Wu, "Accelerated trip of power transmission line based on biorthogonal wavelet analysis", *IEEE Power Engineering Society Summer Meeting*, 2000, vol. 3, pp. 1333-1337.

[16] A. T. Johns, R. K. Aggarwal, Z. Q. Bo, "Non-unit protection technique for EHV transmission systems based on fault-generated noise. Part 1: Signal measurement", *IEE Proceedings on Gener., Transm. & Distrib.*, vol. 141, no. 2, pp. 133-140, Mar. 1994.

[17] A. Sharafi, M. Sanaye-Pasand, and P. Jafarian, "Non-communication protection of parallel transmission lines using breakers open-switching travelling waves", *IET Gener., Transm. & Distrib.*, vol. 6, no. 1, pp. 88-98, Jan. 2012.

[18] D. W. P. Thomas, F. R. F. de Lima, and C. Christopoulos, "A travelling-wave relay for the protection of EHV transmission-lines with teed feeders", *Fifth International Conference on Developments in Power System Protection*, 1993, pp. 232-235.

[19] A. M. Carter, R. K. Aggarwal, A. T. Johns, and Z. Q. Bo, "Computer-aided design of a new non-unit protection scheme for EHV teed circuits", *IEE Proceedings on Gener., Transm. & Distrib.*, vol. 143, no. 2, pp. 142-150, Mar. 1996.

[20] G. Rosas-Ortiz, and T. Sidhu, "Accelerated trip scheme for second zone distance protection in three-terminal lines", *Proceedings of the 1st International Conference on Advanced Power System Automation & Protection (APAP)*, May 2004, Jeju Island, Korea, pp. 272-277.

[21] P. Jafarian, and M. Sanaye-Pasand, "High-frequency transients-based protection of multiterminal transmission lines using the SVM

 ation information: DOI 10.1109/TPWRD.2016.2638544, IEEE

technique," *IEEE Trans. on Power Del.*, vol. 28, no. 1, pp. 188-196, 2013.

[22] V. Leifloff, P. Bastard, "Novel algorithm for accelerated second zone tripping of non-unit distance protection", *Seventh International Conference on Developments in Power System Protection*, 2001, IEE 9-12, pp. 434-437.

[23] P. J. Moore, H. Al-Nasseri, "Improved zone 2 acceleration scheme using sound phase seen impedance", *Eighth IEE International Conference on Developments in Power System Protection*, 2004. vol. 2, pp. 457-460.

[24] G. Rosas-Ortiz, and T. Sidhu, "High-speed backup scheme for zone 2 of non-pilot distance relays", *IET Gener. Transm. & Distrib.*, vol. 1, no. 6, pp. 938–947, Nov. 2007.

[25] K. Takagi, Y. Yomakoshi, M. Yamaura, R. Kondow, and T. Matsushima, "Development of a new type fault locator using the one-terminal voltage and current data," *IEEE Trans. on Power Apparatus & Systems*,vol. PAS-101, no. 8, pp. 2892–2898, Aug. 1982.

[26] P. M. Anderson, *Analysis of Faulted Power Systems*. vol. 445. New York: IEEE press, 1995.

[27] P. Jafarian and M. Sanaye-Pasand, "High-speed superimposed-based protection of series-compensated transmission lines," *IET Gener., Trans. & Dist.*, vol. 5, no. 12, pp. 1290-1300, Dec. 2011.

[28] S. M. Hashemi, M. T. Hagh, and H. Seyedi, "Transmission-line protection: a directional comparison scheme using the average of superimposed components," *IEEE Trans. on Power Del.*, vol. 28, no. 2, pp. 955-964, Apr 2013.

Sadegh Vejdan (S'15) received the B.Sc. and M.Sc. degrees both in electrical engineering from The University of Tehran in 2013 and 2015, respectively. Currently, he is pursuing PhD degree in electrical engineering at the Georgia Institute of Technology, Atlanta, GA, USA. His research interests include power system protection and applications of signal processing techniques in power systems.

Majid Sanaye-Pasand (M'98-SM'05) received the B.Sc. degree in electrical engineering from The University of Tehran, Tehran, Iran, in 1988 and the M.Sc. and Ph.D. degrees in electrical engineering from The University of Calgary, Calgary, AB, Canada, in 1994 and 1998, respectively. Currently, he is a Professor with the School of Electrical and Computer Engineering, University of Tehran, where he is also with the Control and Intelligent Processing Center of Excellence. His research interests include power system protection, control, and transients. Prof. Sanaye-Pasand is an editor of the IEEE TRANSACTIONS ON POWER DELIVERY.

Tarlochan S. Sidhu (M'90-SM'94-F'04) received the Ph.D. degree in electrical engineering from University of Saskatchewan, Saskatchewan, Saskatoon, SK, Canada, in 1989. He is currently a Professor and Dean of Faculty of Engineering and Applied Science at University of Ontario Institute of Technology (UOIT), Oshawa, ON, Canada. Prior to this, he was a Professor and Chair of the Electrical and Computer Engineering Department at the University of Western Ontario, London, ON, Canada. He also has held the NSERC/Hydro One Senior Industrial Research Chair in Power Systems Engineering. His research interests include power system protection, monitoring, control and automation.